Friction and wear of single-crystal silicon at elevated temperatures

D.-S. PARK, S. DANYLUK, M. J. MCNALLAN
University of Illinois at Chicago, Department of Civil Engineering, Mechanics and Metallurgy MC: 246, Box 4348, Chicago, Illinois 60680, USA

Single-crystal silicon wafers ((1 1 1) and (1 0 0)p-type) were abraded at room temperature 300 °C, and 600 °C by a polycrystalline partially stabilized zirconia ball in a ball-on-reciprocating flat geometry. The sliding direction was ⟨1 1 0⟩. The friction coefficient was recorded as a function of reciprocating strokes and the deformation mode of the silicon. The friction coefficient at room temperature decreased with the number of strokes, and this variation was less affected by the number of strokes at the higher temperatures. The wear track width and depth were measured at the three temperatures. Wear increases as the temperature is raised to 300 and 600 °C. Optical and scanning electron microscopy of the subsurface damage reveals that cracks are generated at RT and 300 °C and dislocations are produced at 600 °C. The change in deformation mode with temperature from brittle fracture to plastic deformation accounts for the differences in wear.

1. Introduction
Abrasion and wear are routinely used in the processing of single crystal semiconductors that are fabricated into electronic devices. For example, after single-crystal silicon is grown from the melt, the outside surface is ground into a uniform diameter to facilitate handling and subsequent processing, and a flat is formed along the length of the cylinder to specify the orientation. These single-crystal cylinders are then sliced into wafers. The grinding and wafering are done by high-speed, circular, diamond-impregnated blades and tools that are flooded with lubricants. This mechanical processing generates cracks and dislocations in the subsurface region of the cylinder and wafers, and further processing such as polishing and electroetching is needed to remove this damage because cracks can cause unexpected fracture during heat treatments and handling, and dislocations degrade the electrical properties of unfinished devices.

A good deal of research has been done to quantify the damage in semiconductors produced by abrasion and wear. It has been found that the densities and lengths of microcracks, and the density of the dislocations generated by abrading silicon depends on the loads [1, 2], lubricants [3] and, relative speed and vibration of the tool [4]. It has also been found that silicon undergoes a brittle-to-ductile transition due to tribological contact depending on the fluids [3], load [5]; and temperature [6]. Since abrasive contact is expected to increase the temperature of the silicon, this transition would be expected to have a significant influence on the wear of silicon during mechanical processing.

The present study was initiated in an attempt to describe the ductile-to-brittle transition in single-crystal silicon wafers deformed at elevated temperatures in a geometry in which the stresses, environmental conditions, and materials properties are known. A ball-on-flat geometry was used to abrade silicon surfaces in a linear multiscratch motion in a predetermined crystallographic direction with a partially stabilized zirconia (PSZ) ball. The scratching speed was such that the temperature variability in the wear rate could be attributed predominantly to the environmental conditions. Friction and wear were measured and correlated to the damage morphology.

2. Experimental details
Single-crystal silicon wafers ((1 1 1)p-type and (1 0 0)p-type, 104 mm in diameter and 0.5 mm thick), supplied by the Monsanto Electronic Materials Company, were used in these experiments. The wafers have one face lapped and the other polished according to semiconductor industry standards. The resistivity was 0.21 ohm-cm for the (1 1 1)p-type and 0.31 ohm-cm for the (1 0 0)p-type samples. The wafers were sectioned into 44.5 mm × 19.3 mm rectangular shapes and cleaned wih acetone, trichloroethylene, and methanol prior to abrasion. The specimen abraded at room temperature was additionally heated to 300 °C and cooled to room temperature (RT) in purified argon to preclean the surface [7].

Fig. 1 shows a schematic of the test apparatus. A specimen was situated in a quartz reaction tube inside a furnace and the surface was oriented so that the scratching direction is ⟨1 1 0⟩. The reaction tube was capped with an insulator and copper plate which is cooled by flowing water. Argon gas from the tank is

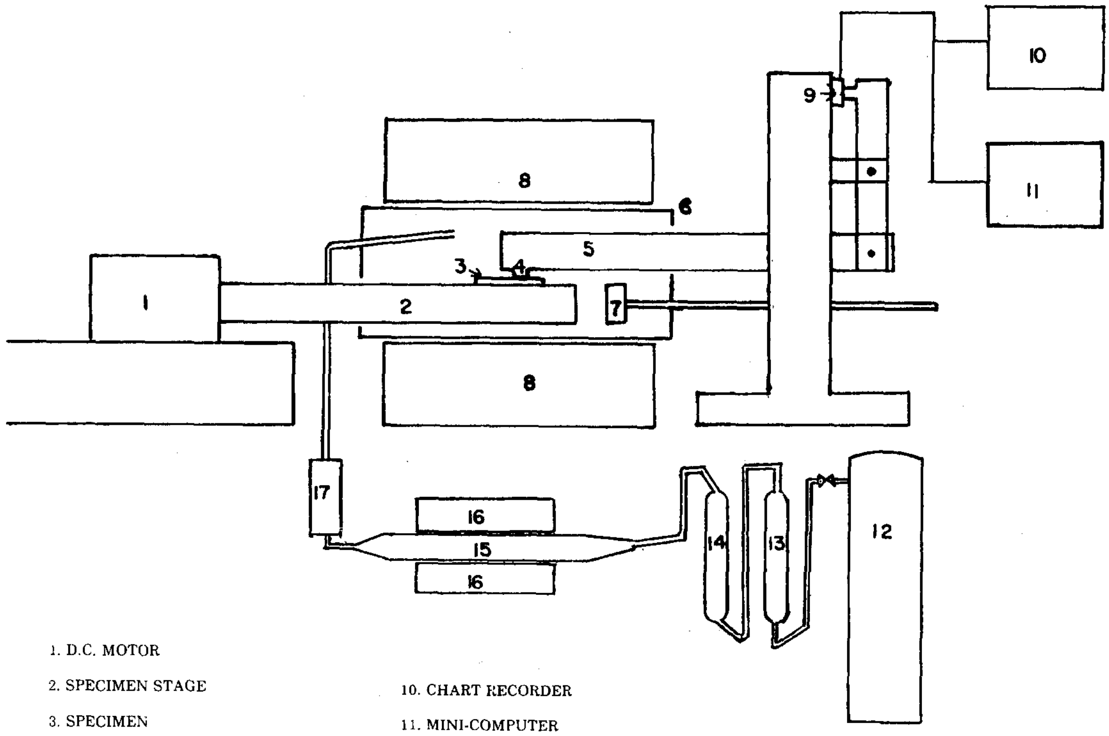

1. D.C. MOTOR
2. SPECIMEN STAGE
3. SPECIMEN
4. HEMISPHERICAL INDENTER
5. INDENTER HOLDER (UPPER ARM)
6. QUARTZ REACTION TUBE
7. SPECIAL WRENCH
8. FURNACE
9. FORCE TRANSDUCER
10. CHART RECORDER
11. MINI-COMPUTER
12. ARGON GAS CYLINDER
13. DRIERITE (MOISTURE REMOVAL)
14. ASCARITE (CO_2 REMOVAL)
15. HOT COPPER WIRE (O_2 REMOVAL)
16. FURNACE
17. FLOW METER

Figure 1 Schematic diagram of the experimental apparatus.

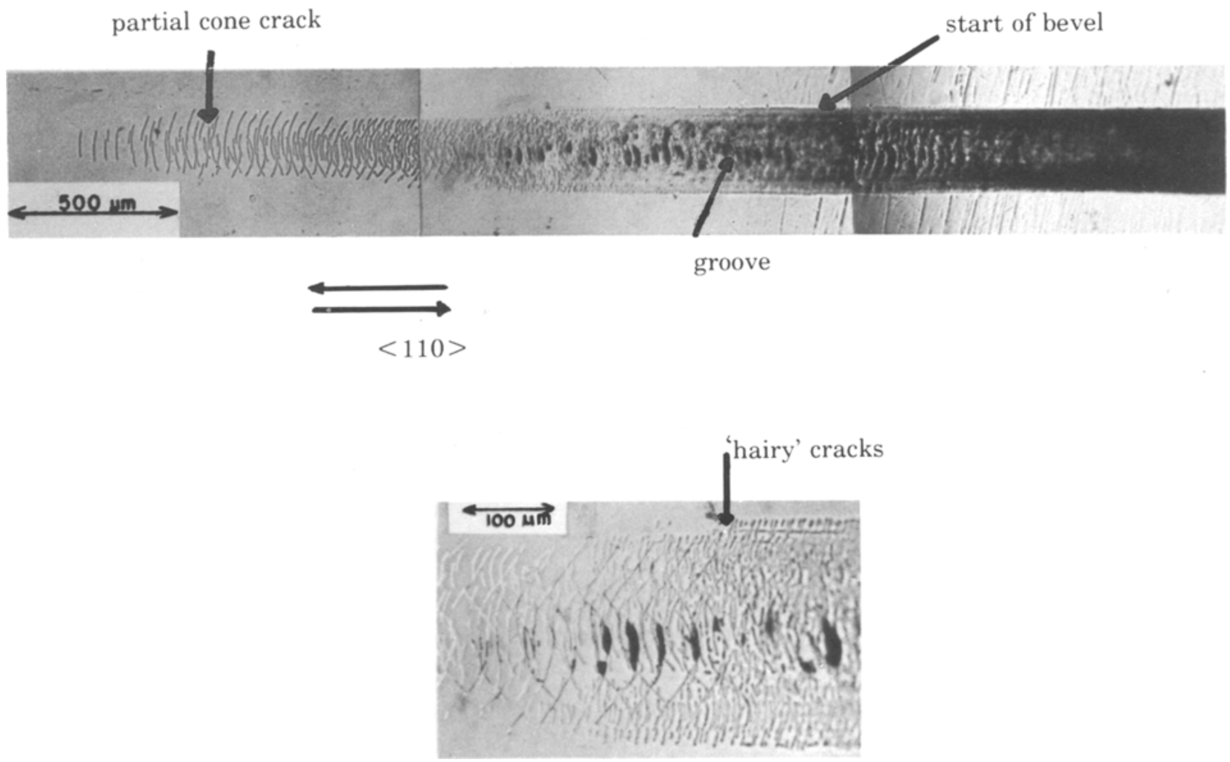

Figure 2 Optical micrographs of the groove and bevel in the (1 1 1)p-type silicon after 100 reciprocating scratches at room temperature. The environment was Ar and the load on the spherical PSZ ball was Ar 4.15 N.

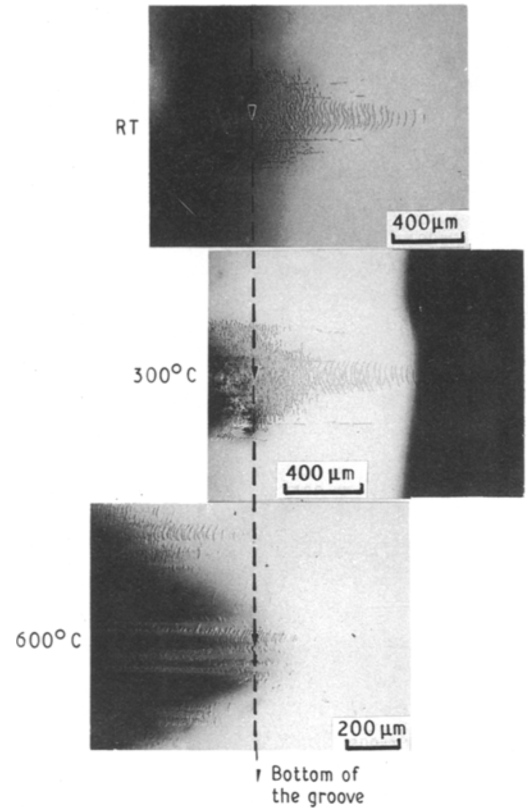

Figure 3 Optical micrograph of the tip of the bevel of the (1 0 0)p-type silicon sample abraded at (a) RT, (b) 300 °C, and (c) 600 °C. The experimental conditions are described in the text.

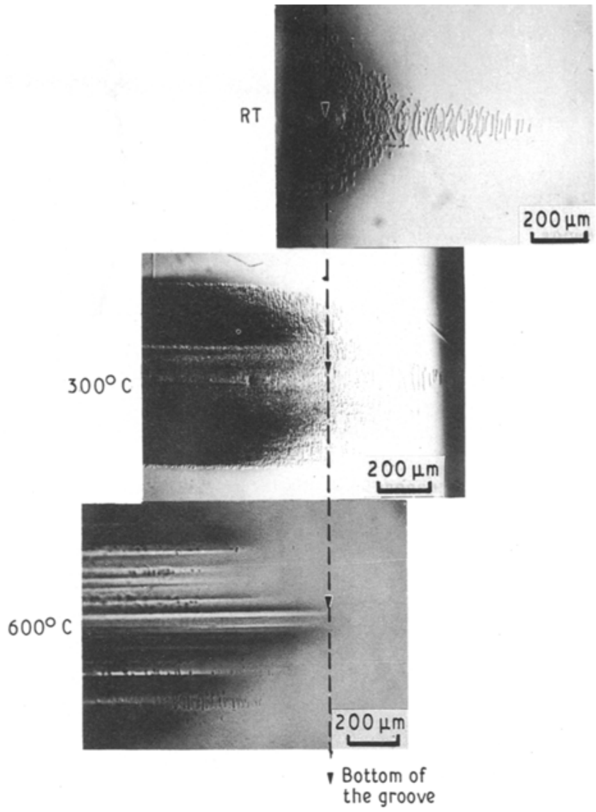

Figure 4 Optical micrograph of the tip of the bevel of the (1 1 1)p-type silicon sample abraded at (a) RT, (b) 300 °C, and (c) 600 °C by a spherical PSZ indentor dead-loaded to 3.67 N. The abrasion was carried out in an Ar environment as described in the text.

passed through drierite for moisture removal, ascarite for CO_2 removal, and hot copper wire for O_2 removal prior to insertion into the reaction tube. The argon flow rate was 3700 cm^3 per minute at room temperature. The sample stage is driven by a direct current (d.c.) motor at a speed that may be adjusted from 5 mm/sec to 10 mm/sec.

The length of travel of the PSZ ball was 21.75 mm. The hemispherical partially stabilized zirconia ball (6.35 mm diameter) dead-loaded to 3.67 N or 4.15 N was mounted in a titanium alloy holder by pressing the ball against the wall of the holder with a screw mount. The pressure induced by the screw compensates for the stress relief due to the difference in thermal expansion between the PSZ ball and the titanium-alloy holder. The friction force between the indentor and the specimen was measured by a transducer (Sensotec Inc., model 31) and recorded by the minicomputer and chart recorder. The sampling rate of the transducer is four data points per second. The signal is converted to a force and a code calculates an average friction coefficient from a measure of 400 data points.

The elevated temperature experiments were carried out by mounting the specimen into the furnace and raising the temperature to 300 °C or 600 °C and stabilizing either temperature to ± 5 °C prior to abrasion. Immediately after the abrasion, the furnace is cooled

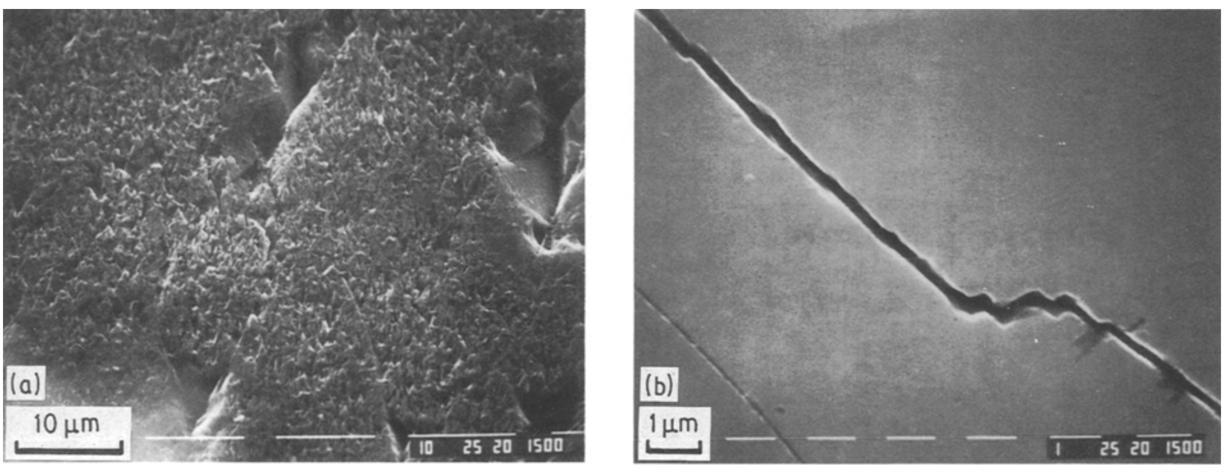

Figure 5 Scanning electron micrograph of (a) the etched wear track and (b) bevel of the (1 0 0) sample abraded at RT.

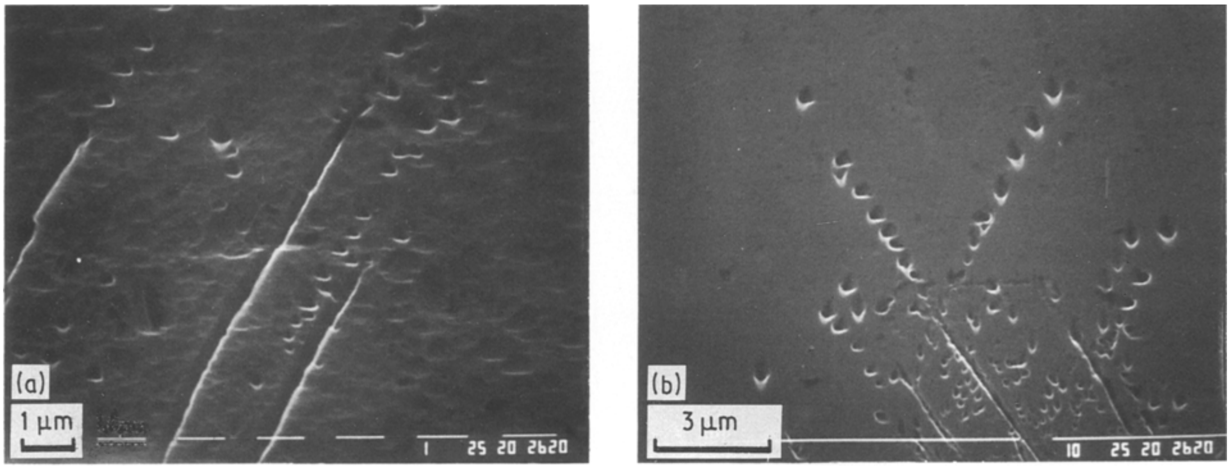

Figure 6 Scanning electron micrograph of (a) the etched wear track and (b) bevel of the (1 1 1) sample abraded at 600 °C.

and the specimen is driven out of the furnace and loosened from the stage. The specimen is then removed from the stage, mounted on the bevel polishing fixture and polished to 0.05 μm alumina powder. A chemo-mechanical polish using Nalco 2350 colloidal silica solution was the final polishing step. The prepared surfaces were then etched in a Sirtl solution which consists of 10 cc or 48% HF, 10 cc of deionized water and 2 g of chromium trioxide.

3. Results

The abrasion of the silicon by the PSZ ball produces a wear groove; the width and depth of which depend on the load and temperature of the experiments. The formation of the wear groove is the result of damage and part of this investigation was to determine the correlation of friction with wear and subsurface damage.

Fig. 2 is an optical micrograph of the bevel-polished region which contains typical examples of the partial cone cracks in the subsurface region of a (1 1 1)p-type wafer after 100 reciprocating strokes. The normal load in this case was 4.15 N and the sliding speed was 5 mm/sec. The friction coefficient was measured to be 0.44. The subsurface depth of the deepest crack in this micrograph is 186 μm below the bottom of the groove. The higher magnification micrograph of the middle portion suggests that wear debris is generated by intersection of the partial cone cracks. The cracks at the perimeter of the groove are shallower than the partial cone cracks and do not appear below 140 μm from the top surface.

The wear depth was measured after the number of strokes was increased to 2500. Fig. 3 shows examples of optical micrographs of a polished and etched area from the bevel region for the samples abraded at RT, 300 and 600 °C. The subsurface has partial cone cracks that extend to 83 and 74 μm below the bottoms of the grooves for the (1 1 1)p-type samples abraded at RT and 300 °C. These depths correspond to 94 and

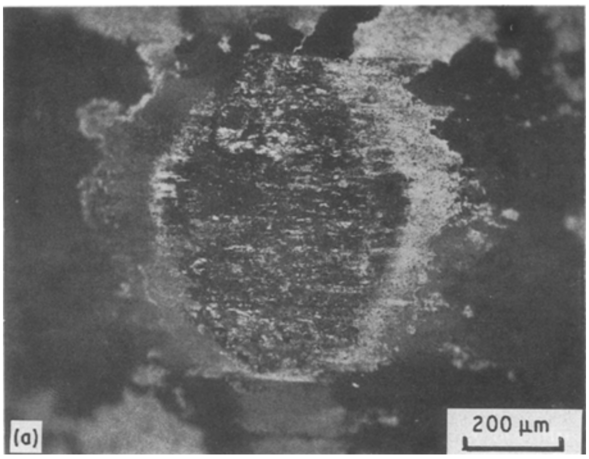

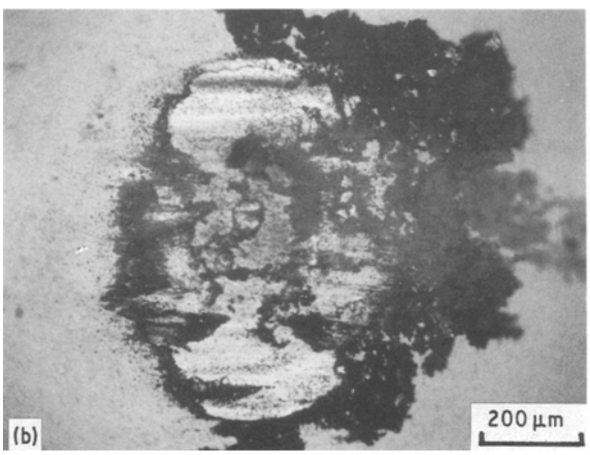

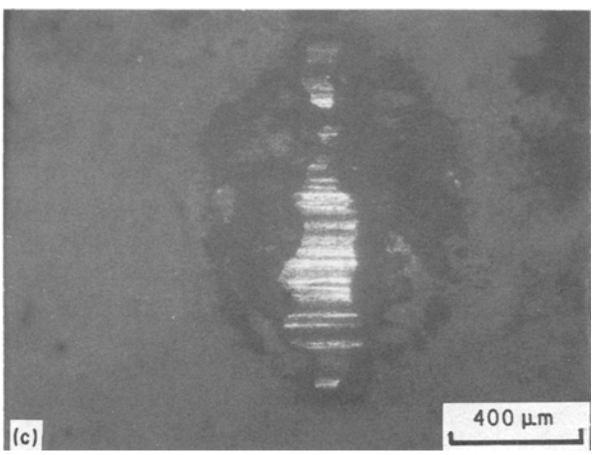

Figure 7 Optical micrograph of the contact area on the PSZ ball used in the (a) RT, (b) 300 °C, and (c) 600 °C experiments.

91 μm from the top surface. There are no gross partial cone cracks for the sample abraded at 600 °C. Micrographs of samples abraded at 600 °C emphasize the change from brittle fracture to plastic deformation. This change in material behaviour becomes more apparent in the (1 0 0)p-type sample as shown in Fig. 4. This figure shows that cracks are not observed for the sample abraded at 600 °C.

Further examination of the damage morphology of the wear track by scanning electron microscopy showed that the room temperature and 300 °C grooves of the (1 1 1)p-type silicon are composed of shallow cracks and partial cone cracks that extend into the bulk of the sample as shown in Fig. 5a. An example of a cone crack in the bevel region is shown in Fig. 5b. This crack changes orientation by jogging along cleavage steps. Scanning electron microscopy of the samples abraded at 600 °C show some evidence of microcracks and dislocations (Fig. 6). These scanning electron micrographs show typical crack tips in the

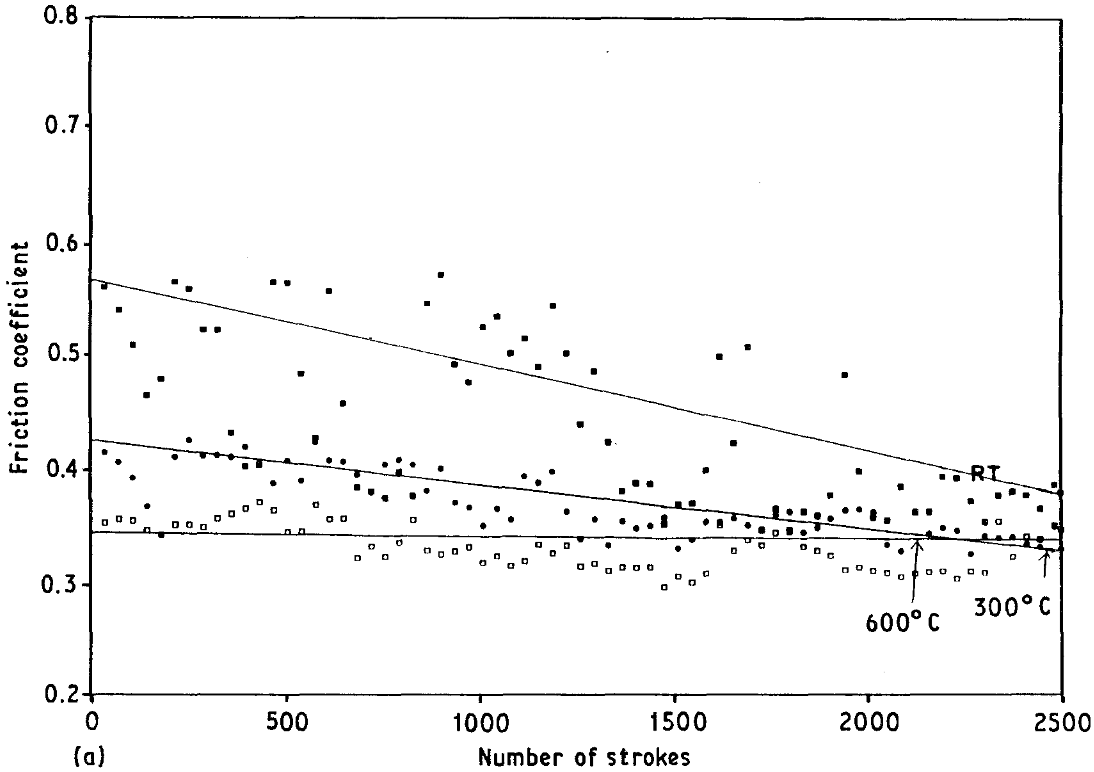

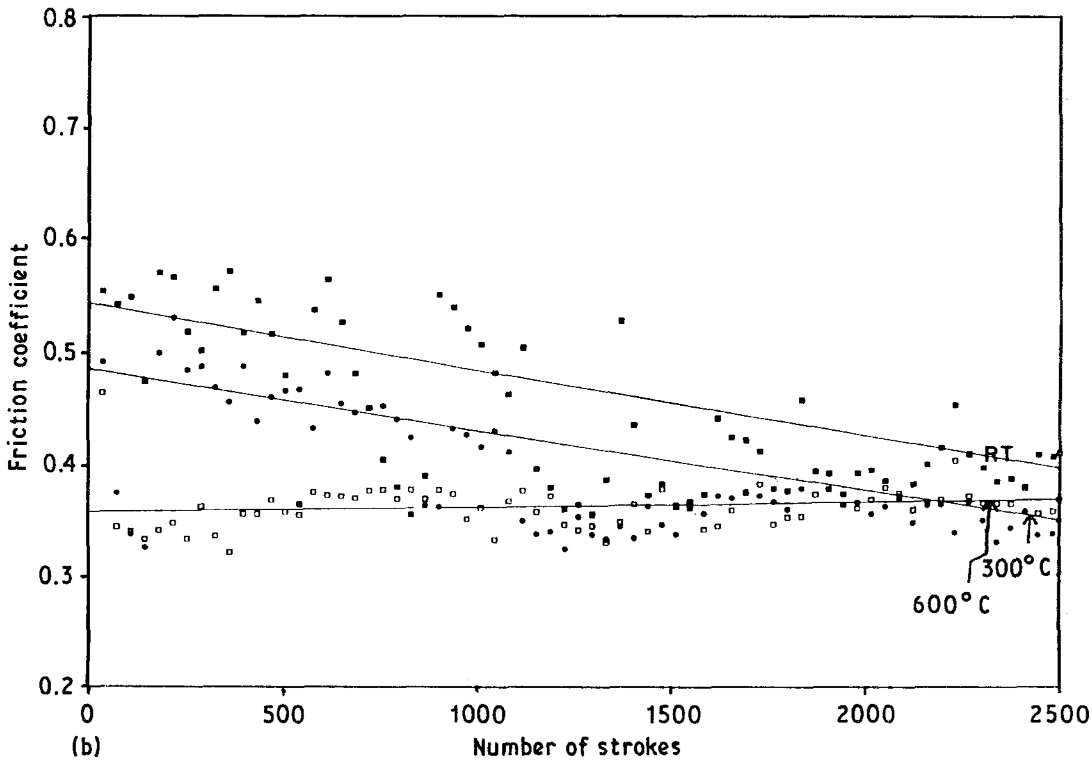

Figure 8 Friction coefficients versus number of reciprocating scratches of the (a) (1 1 1) and (b) (1 0 0)p-type single-crystal silicon abraded by a hemispherical PSZ indentor at RT, 300 °C, 600 °C. The experimental details are given in the text.

bevel region and etch pits emanating from the crack tips. The spacing between etch pits and their distribution indicate that the stresses at the crack tip expel and propagate the dislocations.

Fig. 7 shows typical optical micrographs of the contact area of the PSZ ball after 2500 reciprocating strokes. The PSZ ball is worn into an elliptical shape and the contact area conforms to the wear track width. While the room temperature contact surface is covered with the wear debris, the higher temperature contact surface has a middle strip with lines parallel to the sliding direction. This middle strip is uncovered by debris.

Fig. 8 shows the friction coefficients for these samples. The room temperature friction coefficient of the (1 1 1)p-type sample shows a wide variability and decreases with the number of strokes from 0.57 to 0.42. At 300 °C, the variability of the friction coefficient and its value also decreases with the number of strokes from 0.42 to 0.32. At 600 °C, the friction coefficient shows the least variability and remains unchanged at approximately 0.34. The friction coefficients at low temperatures are high but approach the high temperature value after 2500 strokes. The wear track depth and the wear track width were also measured by optical microscopy. Fig. 9 shows the wear track depth and width as a function of temperature. The wear track depth increases from 11 to 88 μm for the (1 1 1) sample and 12 to 92 μm for the (1 0 0) sample. The increase between 300 and 600 °C is steeper than that between RT and 300 °C.

4. Discussion

The ball-on-flat geometry used in these experiments has been studied for many years, and the stresses induced in elastic, isotropic solids by a sliding spherical indentor are well known [8, 9]. A rough estimate of the stress distributions for these geometries may be obtained by using these prior analyses and the materials parameters for the (1 0 0) surface and [1 1 0] sliding direction in silicon. An example of such a calculation is shown in Fig. 10 where the principal stress, σ_{xx}, divided by the maximum stress σ_{max} is plotted versus the dimensionless distance x/a. Here x is the distance from the central axis of the ball and a is the ball radius. The calculations are shown for friction coefficients of 0.3, 0.5, and 0.7. The variables used in this calculation were as follows: the radius of the PSZ ball was 3.175 mm, and Young's modulus and Poisson's ratio are 2.0×10^{11} MPa and 0.32, respectively. Young's modulus and Poisson's ratio for silicon are 1.11×10^{9} MPa and 0.18 for the [1 1 0] direction [10]. This figure indicates that the stresses vary with the friction coefficient, and compressive stresses develop ahead of the sliding PSZ ball and tensile stresses are generated at the back contact zone. The maximum tensile stress increases from 0.75 to 1.25 as the friction coefficient increases from 0.3 to 0.7. The size of the cone cracks would depend on these tensile stresses, and a comparison of the size of the Hertzian contact circle and the partial cone cracks generated at room temperature are approximately similar, 2×10^{-4} m. This correspondence verifies that the calculations of the extent of the tensile stresses using a linear elastic model are a reasonable approximation to fracture.

As the number of strokes increases and a wear groove is formed, the stresses beneath the ball decrease and the size of the partial cone cracks decreases because the contact area is larger. Fig. 2 shows the decrease in the size of the partial cone cracks along the bevel which is consistent with the fact that the stresses decrease as wear proceeds. The intersection of the cone cracks forms debris and wear is greater at the beginning of the test and decreases as the groove gets deeper. The variability of the friction coefficient for the

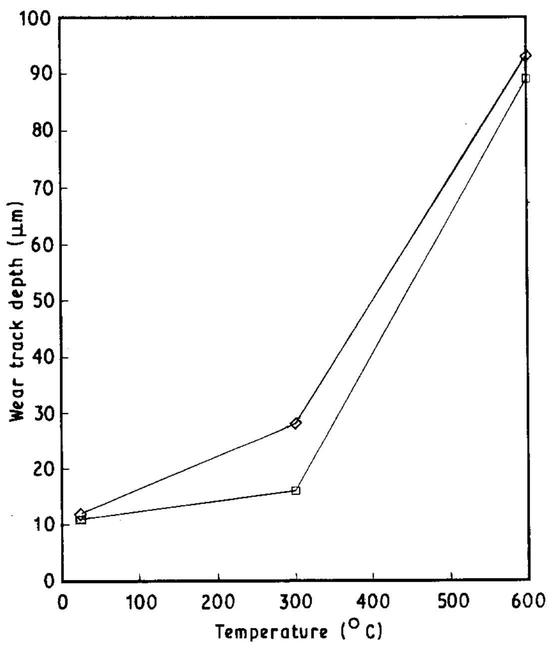

Figure 9 The wear track depth (× 10^{-6} m) versus temperature (°C) for the (1 0 0) (◇) and (1 1 1) (□) single-crystal silicon sample abraded by a hemispherical PSZ indentor.

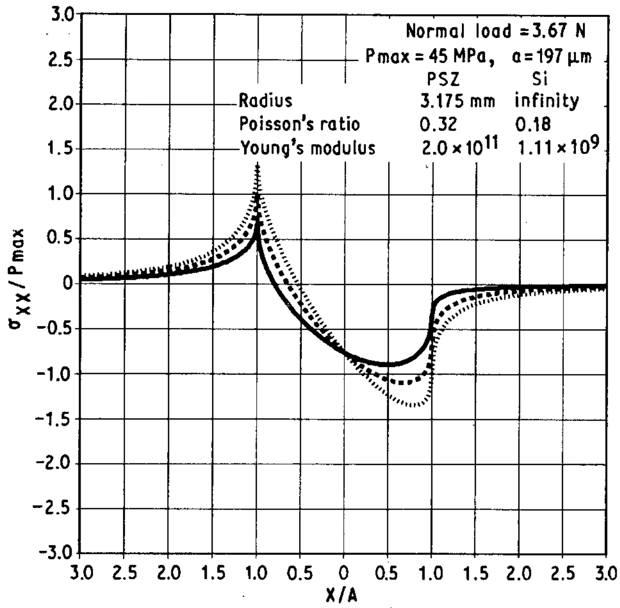

Figure 10 Stress σ_{xx} divided by the maximum stress σ_{max} versus the reduced distance x/a. The friction coefficients were allowed to vary from 0.3 to 0.7. The load on the PSZ indentor was 3.67 N. The physical parameters used in the calculation are given in the text.

room temperature experiments is related to the stresses and the statistics of crack generation.

As the temperature is increased and/or the load is decreased, a brittle-to-ductile transition occurs. Evidence of this transition is shown in Figs 3 and 4, as a decrease in the depth to which the partial cone cracks penetrate beneath the groove surface, and Fig. 6 which shows dislocation etch pits in the (1 1 1)p-type sample. There are two reasons for this transition. Since dislocations are thermally activated, a brittle-to-ductile transition would occur when the Peierls energy becomes smaller than the surface stress associated with cracks. Dislocations in silicon are known to become thermally activated at temperatures greater than 550 °C [11] and our results are consistent with this concept. Secondly, there has been some evidence that a brittle-to-ductile transition is associated with the extent of the stresses as compared to surface charges in semiconductors. For example, there has been some suggestion that silicon goes through a brittle-to-ductile transition as the load on a Vickers indentor is lowered below 0.98 N [5] or when the size of the indentor is decreased [1, 5]. As wear proceeds, stresses may be reduced to below a threshold value where electronic charge carriers affect mechanical deformation [12]. These two effects are reflected in the friction data. The variability in friction decreases as the number of strokes, and temperature increases because the stresses decrease and dislocations become thermally activated.

5. Conclusions

The wear and friction coefficients between a hemispherical partially stabilized zirconia slider and (1 0 0) and (1 1 1)p-type single-crystal silicon were measured. The friction coefficients versus number of strokes show a large variability at RT and 300 °C, but a small variability at 600 °C. The friction coefficient decreased with the number of strokes at RT and 300 °C, from 0.57 to 0.38 and 0.42 to 0.33, respectively. At 600 °C the friction coefficient was independent of the number of strokes, and the variability decreased in all three cases. A brittle-to-ductile transition was observed to occur between 300 and 600 °C. The cracking propensity decreases and dislocation etch pits decorate the wear surface as the temperature is increased from 300 to 600 °C. The brittle-to-ductile transition is probably related to thermal activation of dislocations as the temperature is increased. Electronic space charges may influence wear if local stresses fall below some minimum threshold.

Acknowledgements

This work was supported by the National Science Foundation, Tribology Program, grant number MSM-8714491.

References

1. K. E. PUTTICK, M. A. SHAHID and M. M. HOSSENI, *J. Phys. D* **12** (1979) 875.
2. C. SCOTT, MS Thesis, University of Illinois at Chicago (1987).
3. R. E. CUTHRELL, *J. Mater. Sci.* **20** (1985) 4084.
4. T. S. KUAN, K. K. SHIH, J. A. VECHTEN and W. A. WESTDROP, *J. Electrochem. Soc.* **127** (1980) 1387.
5. S. W. LEE, PhD Thesis University of Illinois at Chicago (1986).
6. S. DANYLUK and S. W. LEE, *J. Appl. Phys.* **64** (1988) 4075.
7. R. S. GATES, S. M. HSU and E. E. KLAUS, "Ceramic Tribology: Methodology and Mechanisms of Alumina Wear", NIST Special Publication 758 (National Institute of Standards and Technology, Washington, DC, 1988) p. 42.
8. G. M. HAMILTON, *J. Mater. Sci.* **22** (1987) 989.
9. S. JAHANMIR and N. P. SUH, *Wear.* **44** (1977) 17.
10. J. J. WORTMAN and R. A. EVANS, *J. Appl. Phys.* **36** (1965) 153.
11. J. L. DEMENT, J. C. DESYER, J. RABIER and P. VEYSSIERE, *Script. Met.* **18** (1984) 41.
12. S. G. ROBERTS, P. PIROUZ and P. B. HIRSCH, *J. Mater. Sci.* **20** (1985) 1739.

Received 4 September 1989
and accepted 19 February 1990